「III-V化合物の電気的及び光学的特性の解析と結晶成長」

Chapter 1. Introduction

GaSb has a band gap of 0.72 eV at room temperature (and 0.81 eV at 35 K) and a cubic lattice constant 6.095 Å that is appreciably larger than for GaAs (5.654 Å) and 0.6% larger than for InAs (6.058 Å). GaSb has a melting point of 712 °C which is substantially lower than the 1240 °C of GaAs.[1] Undoped bulk grown GaSb is *p* type with a hole concentration of the order of 10^{16} ~10^{17} cm^{-3}. The native defect responsible is Ga on an Sb site and a complexes. There is a report that center is doubly ionized with the first and second levels lying 33 and 80 meV above the valence band edge.[2] GaSb is direct band gap material and so of interst for electro optical devices. Liking GaAs, GaSb also exsits a problem to achieve good oxides with low interface state density, high-resistivity, high break-down field strength and suitable for high temperature processing.

Electron mobilities in the range 4000-5000 cm^2/Vs may be expected for 10^{17} cm^{-3} doping in bulk GaSb at 300 K.[3,4] This is comparable to the electron mobilities for GaAs. The hole mobility is 500-600 cm^2/Vs for 4×10^{16} cm^{-3} doping and so tends to be at least as high as for GaAs.[5] Photoluminescence of shallow defects in GaSb has been studied by Nicholas.[6]

The optical properties of GaSb homojunctions have particular potential for high-speed low-noise avalanche photodiode detectors (APDs). The ratio of ionization coefficients of holes and electrons k_p/k_n is large.[6-8] High detectivity has also been reported for $InAs_{0.85}Sb_{0.15}$/InAs detectors in spite of 1% lattice mismatch.[9,10] Detection of longer wavelengths, 8-14 μm, is possible with inter-subband absorption in $Ga_{1-x}Al_xSb$/AlSb superlattices[11]. For the lasers and waveguides,[12-15] the (AlInGa)(AsSb) set of alloys offer excellent performance in the wavelength range 0.8-2.3 μm which includes some atmosphere transmission windows and the 1.3-1.55 μm optical fiber preferred wavelengths. Further improvement may be expected in GaInAsSb injection laser performance since many features found in GaAs laser structure have not yet been thoroughly

explored. This includes quantum wells and graded index confining layers to improve the linewidth and efficiency.[16, 17] Even though large research has been done on this material the device quality material is yet to develop. It is well known that the device-like material is limited by high undoped background carrier density.

In Chapter 2, we have given the detailed process of GaSb growth by MBE. High quality epilayers with excellent morphology were grown.

In Chapter 3, we analyzed the electric transport properties of undoped GaSb. A very detail model is used, which is including various lattice scattering and ionized impurities scattering mechanisms. We found that limitation of device quality is not only high unintentional carrier density, but also high compensation degree in this material. We present the results of the PL and I-V measurement. PL also indicated that high quality epilayers were grown. I-V measurement demonstrated that the tunnel current is dominant at a large temperature region, results from narrow energy band and high carrier density and compensation.

Recently, group III nitride-based semiconductors have emerged as the leading material for short-wavelength optoelectronic devices. The (AlGaIn)N alloy system forms a continuous and direct bandgap semiconductor alloy spaning ultraviolet (UV) to blue/green wavelengths.[18] Unlike Si, GaAs technologies, devices based on group-III nitrides are capable of operating at high temperatures and hostile environments as well as emitters and detectors.[19, 20] As for coherent sources, they are crucial for high density optical read and write technologies. Because the diffraction limited optical storage density increasing roughly quadratically as the probe laser wavelength is reduced, nitride based coherent sources at wavelengths down to UV are attracting a good deal of attention. The recent past and to some extent recent difficulties in growing III-V nitrides manifested themselves as poor crystalline quality and high n-type background carrier concentrations,[21] which resulting from native defects through to by some as nitrogen vacancies. Also, no suitable substrate material with reasonably close lattice match and more stacking order

match could not be easily found. MOCVD has emerged as the leading growth technology for depositing high-quality GaN/InGaN heterostructure-based devices.[22] GaN-based blue LED's with external quantum efficiencies of 10% and 5 mW output power at 20 mA have recently been demonstrated, and the achievement of the shortest wavelength laser diode using InGaN MQW's indicates that these materials have a promising future in optical recording and displays.[23] In oder for further development of these materials to be realized, doping incorporation (especially *p*-type) and ohmic contact technologies to *p*-type material have to be improved.

But such material and related optoelectrical devices are still in the preliminary stage, and many physical mechanisms affecting their active medium behavior are not understood in detail.

Due to the large exciton binding energy (27.5 meV) of GaN, which is larger than room temperature (26 meV), and with wide band-gap and small exciton radius (2.76 nm, comparing to screening length K_D^{-1}=2.6 nm, at 10^{18} cm^{-3}) (screening effect will be reduced), the many body effect is very important for this material.

In Chapter 4, we investigated the band-gap narrowing of current injected InGaN/AlGaN surface emitting diode, caused by many body effect.

The development of group III nitride-based short-wavelength lasters may make them the best potential optical devices to complete the optical computation. Optical bistable and nonlinear devices have many advantage for applications in optical logic and signal processing. In Chapter 5, the thermo-optical nonlinearity was studied. This material demonstrated very large thermo-optical nonlinearity near band-gap edge, the thermo-optical coefficient increases with increasing the temperature. Kramers-Kronging transformation was used to verify our results, a qualitative consistency was obtained.

Finally, in Chapter 6, we outline the conclusions drawn from this work.

Reference

[1]R. C. Sharma, T. Leo Ngai and Y. A. Chang, J. Ellectron. Mater. 16, 307 (1987).

[2]R. P. Nanavati and M. Eisencraft, Proc. Int. Conf. on the Phsics of Semiconductors, Kyoto, 1966, J. Phys. Soc. Japan 21, Suppl., 603 (1966).

[3]M. E. Lee, I. Poole, W. S. Truscott, I. R. Cleverley, K. E. Singer and D. M. Rohlfing, J. Appl. Phys. 68, 131 (1990).

[4]O. Madelung, *Phyiscs of III-V Compounds.* Wiley, New York (1964).

[5]D. J. Nicholas, M Lee, B. Hamilton and K. E. Singer, J. Cryst. Growth 81, 298 (1987).

[6]H. Luquet, M. Perotin, L. Gouskov, C. Llinares, H. Archidi, M. Lahbadi, M. Karim and B. Mbov, J. Appl. Phys. 68, 3861 (1990).

[7]S. Miura, T. Mikawa, H. Kuwatsuka, N. Yasuoka, T. Tanahashi and O. Wada, Appl. Phys. Lett. 54, 2422 (1989).

[8]I. A. Andreev, A. N. Baranov, M. Z. Zhingarev, V. I. Korol'kov, M. P. Mikhailova and Y. P. Yakovlev, Sov. Phys. Semicond. 19, 987 (1985).

[9]S. M. Bedair, J. Electrochem.Soc. 22, 1150 (1975).

[10]A. M. Fox, A. C. Maciel, J. F. Ryan and T. Kerr, Appl. Phys. Lett. 51, 430 (1987).

[11]H. Xie, J. Piao, J. Katz and W. I. Wang, J. Appl. Phys. 70, 3152 (1991).

[12]C. Alibert, M. Skouri, A. Joullie, M. Benouna and S. Sadiq, J. Appl. Phys. 69, 3208 (1991).

[13]T. H. Wood, E. C. Carr, C. A. Burrus, R. S. Tucker, T. H. Chiu and W.-T. Tsang, Electron. Lett. 23, 540 (1987).

[14]Y. Horikoshi, Semiconductors and Semimetals, Vol. 22, Part C, p. 93. Academic Press, New York (1985).

[15]S. Adachi, J. Appl. Phys. 61, 4869 (1987).

[16]N. Toba and K. Nosu, Electron. Lett. 23, 188 (1986).

[17]A. N. Baranov, Appl. Phys. Lett. 59, 2360 (1991).

[18]S. Nakamura, M. Senoh, S. I. Nagahama, N. Iwasa, T. Yamada, T. Matsushita, H. Kiyoku and Y. Sugimoto, Jpn. J. Appl. Phys., Part2 35, L74 (1996).

[19]S. Nakamura, T. Mukai, and M. Senoh, Appl. Phys. Lett., 64, 1687 (1994).

[20]M. A. Khan, D. T. Olson, J. N. Kuznia and W. E. Carlos, J. Appl. Phys. 74 5901 (1993).

[21]S. Nakamura, N. Iwasa, M. Senoh, S. I. Nagahama, T. Yamada and T. Mukai, Jpn. J. Appl. Phys. Lett. 34, L1332 (1995).

[22]S. Nakamura, T. Mukai, and M. Senoh, Jpn. J. Appl. Phys. Lett. 31, 2883 (1992).

[23]S. N. Mohammad, A. A. Salvador, and H. Morkoc, Proc. IEEE. 83, 1306 (1995).

Chapter 2. MBE Apparatus and GaSb Epitaxial Growth

2.1 Introduction

Molecular beam epitaxy (MBE) is a versatile technique for thin epitaxial semiconductor structures, optical and microwave devices preparing.[1-3] In MBE, thin films crystallizes via reactions between thermal atomic and molecular beam and a heated substrate under ultra-high vacuum (UHV) conditions. The composition of the grown epilayer and its doping level depend on the evaporation rates of the appropriate sources. The film growth rate is typically 0.5 -1.0 μm/h. It is chosen low enough that dissociation and migration of the impinging species on the growing surface to the appropriate lattice sites are ensured without incorporating crystalline defects. Consequently, the surface of the grown film is very smooth. Due to the slow growth rate, change in composition and doping can thus be abrupt on an atomic scale alternative wording the eptaxial layers can be grown in atomic layer upon atomic layer.

The MBE mainly distinguishes from previous vacuum deposition techniques is:

1) MBE can significantly more precisely control the fluxes and growth conditions, due to its slow growth rate (0.2~1 μm/h).

2) Because of the vacuum deposition, MBE growth is carried out under conditions far from thermodynamic equilibrium and is governed mainly by the kinetics of the surface processes occurring when the impinging beam react with the outermost atomic layers of the substrate crystal. This is in contrast to other epitaxy growth techniques, such as liquid phase epitaxy (LPE) or vapor phase epitaxy (VPE), which proceed at conditions near thermodynamic equilibrium and are most frequently controlled by diffusion processes occurring in the crystallizing phase surrounding the substrate crystal.

3) Crystal growth can be carried out by MBE at lower temperature than other epitaxy growth techniques (i.e. LPE and VPE)

4) Simple mechanical shutters in front of the beam sources are used to interrupt the beam fluxes, therefore, very abrupt composition and doping profiles are possible.

5) MBE is realized in an ultrahigh vacuum environment, it may be controlled *in situ* by surface sensitive diagnostic methods such as reflection high energy electron diffraction (RHEED), Auger electron spectroscopy (AES) or ellipsometry. These powerful facilitie for control and analysis eliminate much of the guesswork in MBE, and enable the fabrication of sophisticated device structures using this growth technique.

2.2. MBE apparatus

The advanced MBE system mostly consists of three basic UHV building blocks, i.e. the growth chamber, the sample preparation chamber, and load-lock chamber, which are independently pumped and interconnected via large-diameter channels and isolation valves. Therefore the UHV can be maintained while changing substrate. The substrates can be moved between the chambers using magnetically coupled transfer rods. A liquid-nitrogen-cooled shroud is used to enclose the entire growth area in order to condense the residual water vapor and carbon-containing gases in the growth chamber during epitaxy. The substrate holder can rotate continuously to achieve extremely uniform epitaxial layer. Our MBE growth chamber for III-V compounds is shown in Fig. 2-1, which is pumped to a pressure of approximately 10^{-9} Torr after extensive bake out (200 °C, 72 h). Rough pumping is achieved using rotary pumps. Then liquid nitrogen cooled, Ti sublimation pump, turbo molecular pump, ion pump and diffusion pump are used to perform final UHV pump.

The growth systems are equipped with *in situ* surface analytical techniques. The most common facilities in the growth chamber are a quadupole mass spectrometer, which is convenient to have for detecting a leak in the vacuum system or to measure the water vapor background in the residual gas at all times, and a reflection high energy electron diffraction

(RHEED) system, which gives important information about surface cleanliness, structure and proper growth conditions.

The experimental geometry of RHEED is illustrated in Fig. 2-2. Electron having energy of typically 5-50 keV are incident on the substrate in a small glancing angle (1-3°) reflection mode. The diffraction pattern on the fluorescent screen mostly taken in [110] azimuth of (100) oriented substrate, contains information from the topmost layers of the deposited material and it can thus be related to the topography and structure of the growing surface. The diffraction would give streaks perpendicular to the shadow edge of the pattern, the spot diffraction implies that the surface texture is rough and the diffraction is from transmission through the protuberances. Additional features in RHEED pattern at fractional intervals between the bulk diffraction streaks manifest the existence of specific surface reconstruction, which are correlated to the surface stoichiometry and thus directly to MBE growth conditions. Figure 2-3 shows a diffraction in the [110] azimuth of the reconstructed GaSb (1×3) surface. The threefold periodicity is evident from the appearance of fractional-order (1/3, 2/3) streaks between the integral- order streaks, the surface structure depends on the incident fluxes of Ga and Sb as well as the substrate temperature.[4] The (1×3) surface is usually adopted for crystal growth.

Another characteristic feature of RHEED pattern is the existence of periodic intensity oscillations during MBE growth.[5] The period of these oscillations corresponds exactly to the time required to deposit a lattice plane of epitaxial layer. It can be used to calibrate beam fluxes and control alloy composition and the thickness of quantum wells and superlattice layers.

2.3. The process of GaSb growth

GaSb (001) and GaAs (001) substrate are first organically cleaned with trichloroethane, acetone and methanol sequentially. After rinsing in deionized water, for GaSb,the substrate is then etched in solutions of $CH_3COOH:HNO_3:HF$=20:9:1 at room temperature for 40 sec., rinsed

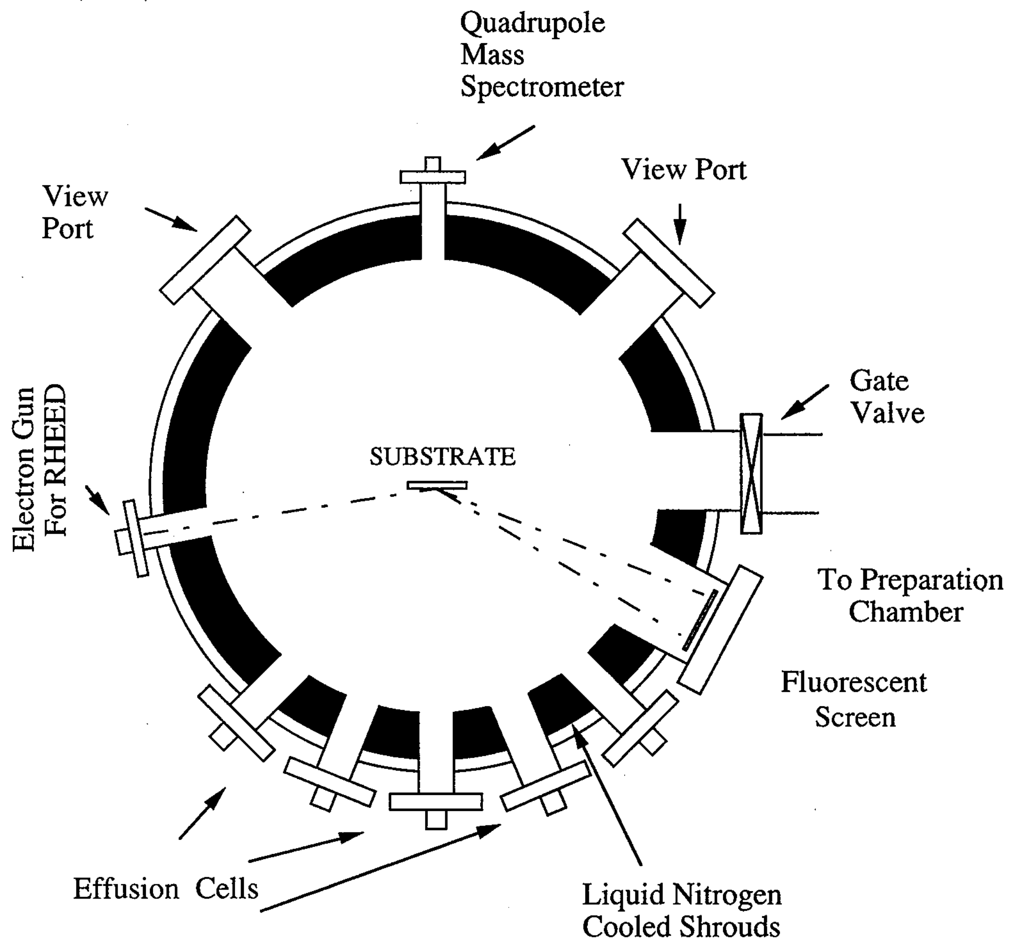

Fig. 2-1 Schematic cross-section of MBE growth champer.

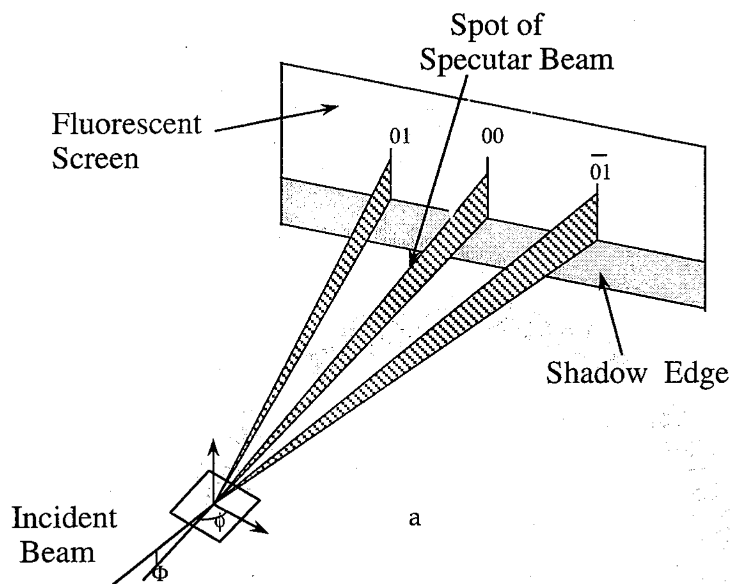

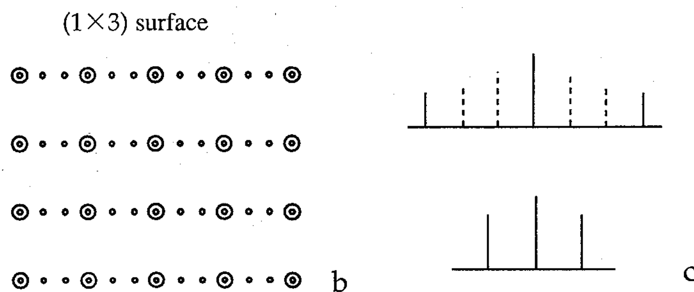

Fig. 2-2 Schematic diagram of RHEED geometry with grazing-angle incidence used as *in situ* analytical tool in MBE (a); Surface unit cell (b); diffraction patterns of (1 × 3) reconstruction.

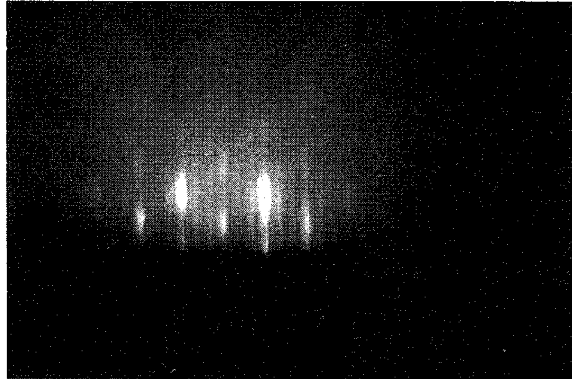

Fig. 2-3 Diffraction pattern from the GaSb (001)-(1 × 3) surface, the [110] azimuth, taken at an electron energy of 20 keV.

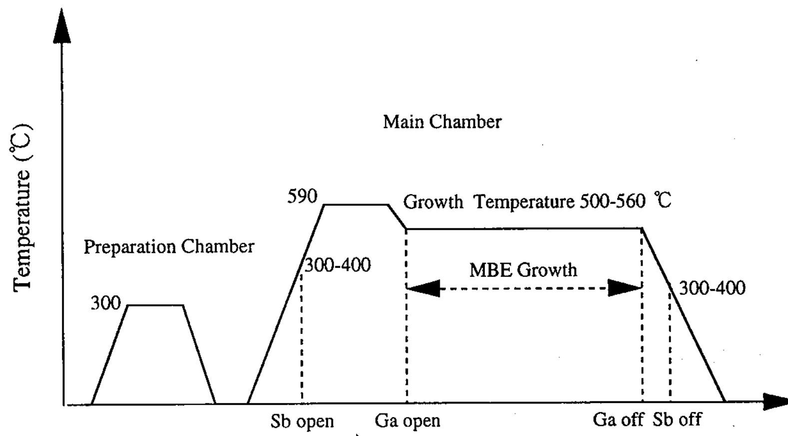

Fig. 2-4 Growth sequence of GaSb.

again in deionized water and then etched in $HCl:HNO_3$=30:1 (at 5 °C for 5 min.), for GaAs is etched in solutions of $H_2O:H_2O_2:H_2SO_4$=1:1:5 at room temperature for 2 min., to remove any oxide and organic materials on the substrate surface. Finally it is rinsed in deionized water for passivation [3] and blow dried with filtered nitrogen gas, the passivated oxide layer serves as a protection for the freshly chemically etched substrate from atmospheric contamination before epitaxial growth. The substrate is then mounted on a preheated (160°C) molybdenum sample holder with indium solder and load into the MBE system immediately. To grow high quality epitaxial layers, one must take meticulous care in substrate preparation, all above operation should perform in a clean ambiance and the MBE system has to be leak-free.

The epitaxial growth sequence of GaSb is shown in Fig. 2-4. After a pump down of 10^{-7} Torr, the substrate were transferred to the preparation chamber and heated to 300 °C for 15 min. to be rid of moisture and air bubbles trapped in the In. Then the sample is entered to growth chamber, after the MBE system is pumped down , the liquid nitrogen shroud cooled and the effusion cells heated to the desired temperature (for Ga at 1000 °C; for Sb at 380 °C). In order for oxide desorption and surface reconstruction, the substrate is heated at 590 °C for 30 min. in antimony ambiance. At this point, the substrate is nearly atomically clean and ready for epitaxial growth. Next, the Ga beam is opened to begin the epitaxial growth.

The basic process for MBE epitaxial growth of III-V semiconductor consists of a co-evaporation of the constituent elements of the epitaxial layer and of dopants onto the heated substrate where react chemically UHV conditions. The composition of the layer and its doping level depend mainly on the relative arrival rates of the constituent elements which in turn depend on the evaporation rates of the respective sources.

Joyce and coworkers [6] have described the kinetic processes leading to the growth of GaAs from Ga and As_2 or As_4 molecules. The group III elements are always supplied as monomers by evaporation from the respective liquid element, and they have a unity sticking coefficient over most of the substrate temperature range used for film growth (500-630°C). The group V

elements that are supplied as tetramers or dimers are more complex. It was found that, in general, group V molecular stick only when group III elements adatom plane are already established. The stoichiometric III-V semiconductors can be grown over a wide range of substrate temperature as long as excess group V molecular are impinging on the growing surface. The excess group V molecular do not stick on the substrate, and the growth rate of the film is only determined by the flux of the group III elements beam. The model is also valid for GaSb, a number of other III-V compounds. According to the model, under excess Sb/Ga flux ratios (5~10), substrate temperature over 430~530°C range, we have grown single crystalline GaSb, while the Ga beam flux was controlled to give a growth rate of 0.76 μm/h. A good control of ternary III-III-V alloys can be achieved by supplying excess group V elements and adjusting the flux densities of the impinging group III beams. Unintentionally doped GaSb which growth by MBE is *p*-type. The Hall effect was measured using van der Pauw method for the epitaxial GaSb layer grown on SI GaAs substrate. The hole mobility and density are 2700 cm^2/Vs and 2.0×10^{16} cm^{-3} at 77 K, and 630 cm^2/Vs, 1.5×10^{17} cm^{-3} at 300 K, respectively. The mobility is high as that reported by other workers.[7] Photoluminscence (PL) spectra of MBE-grown GaSb on undoped GaSb substrate was also studied, PL spectra implies that the epilayer have a good crystalline (PL measurement will be described on Chapter 3 in detail).

2.4. Conclusion

The MBE apparatus and growth process of GaSb were described in detail. It was found that mirror-like surface of GaSb epilayer can be obtained over large substrate temperature range (430~530°C), and Sb/Ga flux ratios (5~10). High quality epilayers with excellent morphology were grown.

References

[1]L. L. Chang, K. Ploog (eds.): *Molecular Beam Epitaxy and Heterostructures*, NATO ASI ser., ser. E, no. 87 (Martinus Nijhoff, Dodrecht 1985).

[2]E. H. C. parker (ed.): *The Technology and physics of Molecular Beam Epitaxy* (Plenum, New York 1985).

[3]M. A. Herman and H. Sitter, *Molecular Beam Epitaxy*, Fundamentals and current status, springer-verlay. Springer Ser. Matter. Sci. 7. Berlin (1989).

[4]A. Y. Cho, and I. Hayashi, Solid State Electron. **14**, 125 (1971).

[5]B. A. Joyce Rep. Prog. Phys. **48**, 1637 (1985)

[6]A. Y. Cho, and H. C. Casey, Appl. Phys. Lett. **25**, 288 (1974).

[7]F. Hatami, N. N. Ledentsov and M. Grundmann, Appl. Phys. Lett. **67**, 656 (1995)